# High-spin states of $^{83}$Rb

W. Gast, K. Dey, A. Gelberg, U. Kaup, F. Paar, R. Richter, K. O. Zell, and P. von Brentano
*Institut für Kernphysik der Universität zu Köln, D-5000 Köln 41, West Germany*
(Received 26 November 1979)

The decay scheme of $^{83}$Rb was studied by gamma-ray spectroscopy with the $^{81}$Br$(\alpha,2n)^{83}$Rb, $^{70}$Zn$(^{16}$O$,p2n)^{83}$Rb, $^{74}$Ge$(^{12}$C$,p2n)^{83}$Rb, and $^{80}$Se$(^{6}$Li$,3n)^{83}$Rb reactions. New energy levels and spins and parities were established. A stretched spin band built on the isomeric $9/2^+$ level at 42.3 keV, a $5/2^-$ ground state quasirotational band, and a three-quasiparticle band were found.

[NUCLEAR REACTIONS $^{81}$Br$(\alpha,2n)$, $E_\alpha$ = 19–25 MeV, $^{80}$Se$(^6$Li$,3n)$, $E_{^6\mathrm{Li}}$ = 23–29 MeV, measured $E_\gamma$, $I_\gamma$, $\gamma$-$\gamma$-coincidence, $\gamma$-angular distribution, $^{70}$Zn$(^{16}$O$,p2n)^{83}$Rb, $E_{^{16}\mathrm{O}}$ = 52 MeV, $^{74}$Ge$(^{12}$C$,p2n)^{83}$Rb, $E_{^{12}\mathrm{C}}$ = 35–49 MeV, measured $E_\gamma$, $^{83}$Rb deduced levels, $J$, $\pi$. Enriched targets, Ge(Li).]

## I. INTRODUCTION

The low-spin states of $^{83}$Rb have been studied in the $\beta$ decay of $^{83}$Sr by Broda *et al.*[1] and by Etherton *et al.*[2] The following attempts to describe these states have been made: Paradellis and Hontzeas[3] and Krishan, Basu, and Sen[4] have calculated the level structure of $^{83}$Rb in a quasiparticle-phonon coupling model which couples the single-proton motion to the vibrations of the neighboring even core. On the other hand, the quite large quadrupole moment compared with the single-particle shell model and the collective vibrator estimate (Table I) are a sign of static deformation. Therefore Scholz and Malik[7] tried to explain the $^{83}$Rb low-lying states by means of the Coriolis coupling model with the incorporation of a residual interaction of the pairing type.

The occurrence of decoupled high-spin states is another effect of the Coriolis interaction. Such decoupled states were found and successfully described in terms of the rotational aligned coupling model (RAC) proposed by Stephens *et al.*[8] in some other transitional $g_{9/2}$ nuclei, e.g., $^{77}$Br,[9] $^{71,73}$As,[10] and $^{81}$Rb.[11] This suggests that, although the even mass nuclei in this region rather show properties of soft nuclei,[12] the high-spin states of adjacent odd neighbors have a more pronounced rotational behavior. Our aim was to get information on high-spin states also for $^{83}$Rb.

TABLE I. Comparison of theoretical and experimental values of the $^{83}$Rb quadrupole moment ($Q$ in $10^{-24}$ cm$^2$) (Refs. 5 and 6).

| | $Q_{\text{single particle}}$ | $Q_{\text{rot. vibrations}}$ | $Q_{\text{experiment}}$ |
|---|---|---|---|
| $^{83}$Rb | 0.096 | 0.19 | 0.27 |

## II. EXPERIMENTAL METHODS AND DATA ANALYSIS

A list of experiments, reactions, and targets is given in Table II. The beams were provided by the FN tandem Van de Graaff accelerator in Cologne. The Ge(Li) detectors used in the experiments were a detector with about 5.4% effeciency at 1.3 MeV gamma rays and a resolution of 1.8 and 1.0 keV at $E_\gamma$ = 1.3 and 0.34 MeV, respectively, and two detectors with about 12% efficiency for $^{60}$Co and a resolution of 2.2 keV at $E_\gamma$ = 1.3 MeV and 1.2 keV at $E_\gamma$ = 0.34 MeV. The energy calibration was done with standard sources and the efficiency calibration with $^{152}$Eu, $^{182}$Ta, and $^{226}$Ra sources. The peak areas and positions were determined by the least-square fit program DAT1.[13]

(1) *The gamma-gamma-coincidence measurements.* The measurements were carried out with the two large volumed detectors each placed perpendicular to the beam axis at 2 cm distance from the target. A conventional slow-fast coincidence system was used with a time resolution of about 15 ns. Typical counting rates in each counter were about 8 kHz. The coincidence acquisition rate was found to be about 1500 Hz. The signals were fed into a PDP 11/20 computer system working as a $3\times4096$ multichannel analyzer which stored each coincidence triplet $(E1, E2, \Delta t)$ on magnetic tape in the event-by-event recording mode during the measurement. A PDP 11/45 computer was used off-line, to set gates on all peaks seen in the projection spectrum as well as a time window (45 ns) on the prompt peak, and to generate the corresponding coincident spectra. Spectra gated with background regions in the vicinity of the peaks were subtracted from the spectra gated with the peaks to reduce the background from Compton tails. The projections (spectra coincident with

 

TABLE II. List of experiments, reactions, and targets used.

| Measurement | Reaction | Beam energy (MeV) | Element (compound) | Target Enrichment (%) | Target Thickness ($mg/cm^2$) | Gold backing thickness ($mg/cm^2$) |
|---|---|---|---|---|---|---|
| $\gamma$-$\gamma$ coin. | $(\alpha, 2n)$ | 23 | $Tl^{81}Br$ | 97.8 | 2 | |
| $\gamma$-$\gamma$ coin. | $(^6Li, 3n)$ | 25 | $^{80}Se$ | 90.2 | 0.7 | 1+4 [a] |
| $\gamma$-excitation | $(^6Li, 3n)$ | 23, 25, 27, 29 | $^{80}Se$ | 90.2 | 0.7 [b] | |
| $\gamma$-ang. dist. | $(\alpha, 2n)$ | 23 | $Tl^{81}Br$ | 97.8 | 4 | |
| $\gamma$-ang. dist. | $(^6Li, 3n)$ | 27 | $^{80}Se$ | 90.2 | 2 | 1+4 [a] |
| $\gamma$-singles [c] | $(^{12}C, p2n)$ | 35–49 | $^{74}Ge$ | 97.8 | 0.9 | 4 |
| $\gamma$-singles [c] | $(^{16}O, p2n)$ | 52 | $^{70}Zn$ | 44.9 | 1 | 4 |

[a] Sandwich.
[b] Rotating target.
[c] No further experiments have been done as the spectra have too many lines from competing reactions.

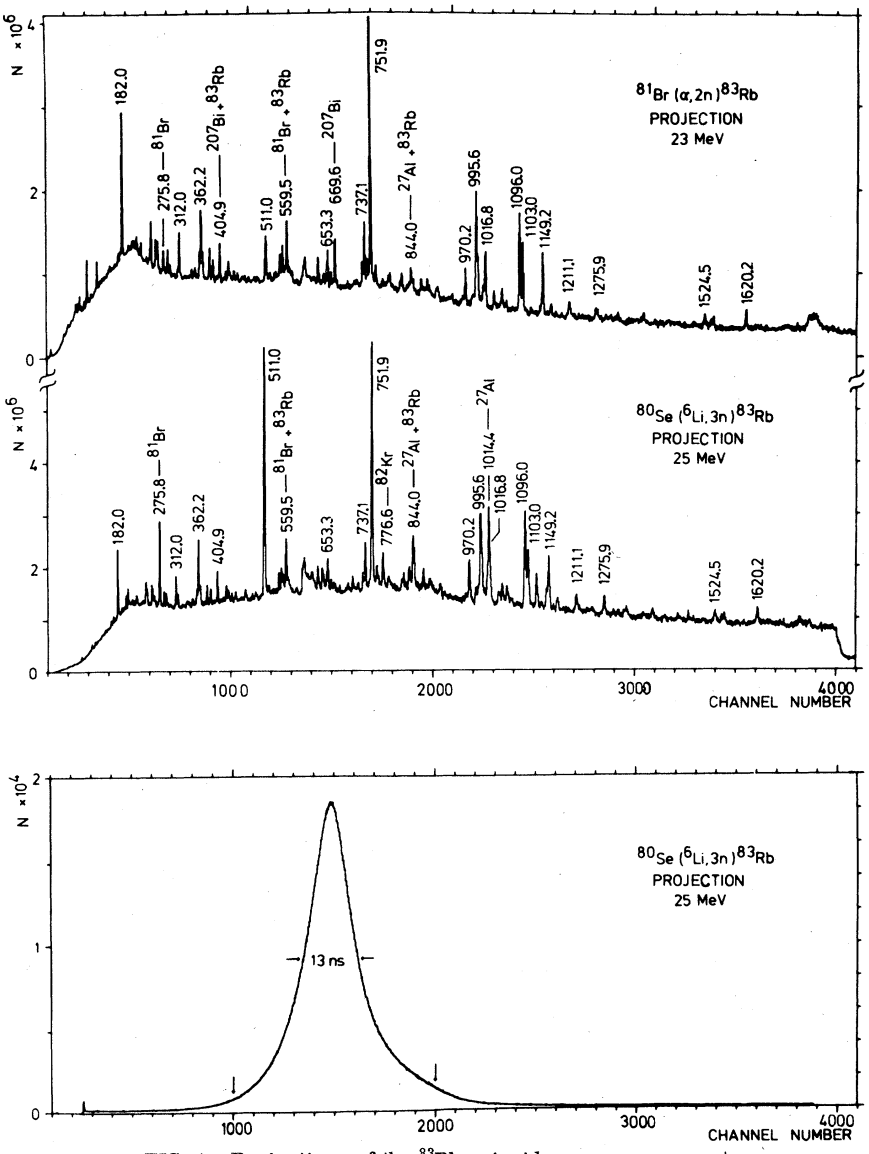


FIG. 1. Projections of the $^{83}Rb$ coincidence measurement.

all events in the other detector) are shown in Fig. 1. Table III gives the gamma-gamma coincidences for the alpha-induced reaction.

(2) *Gamma-ray excitation functions and angular distributions.* These were carried out with two Ge(Li) detectors mounted on the arms of a precision goniometer at a distance of about 25 cm from the target. The excitation functions were measured at 125 and 55° to the beam. The relative normalization was provided by the integrated beam charge. Deadtime corrections were performed using a pulser triggered by the beam. The angular distribution of the $\gamma$ rays following the $(\alpha, 2n)$ reaction was measured at 93.5, 117.5, 128.5, 138.5, 149.5, and 161.5° relative to the beam. The normalization was done using the areas of some well resolved peaks collected in the second counter positioned at 270°. The angular distribution measured with the $(^6\mathrm{Li}, 3n)$ reaction was taken at 40, 75, 90, 113, 125, 135, 145, and 160°. The normalization of this angular distribution was done using the isotropic 260.1 keV line which depopulates the isomeric ($T_{1/2} = 36$ μs)$\frac{9}{2}^+$ level in $^{81}$Br (Ref. 14) [$^{80}\mathrm{Se}(^6\mathrm{Li}, \alpha n)^{81}\mathrm{Br}$ reaction]. The experimental points were fitted to the function

$$W(\theta) = A_0 + A_2 P_2(\cos\theta) + A_4 P_4(\cos\theta), \qquad (1)$$

with $A_2/A_0 = \alpha_2 A_2^{\max}$ and $A_4/A_0 = \alpha_4 A_4^{\max}$, using the symbols of Ref. 15. The free parameters are $\delta$ and $\alpha_2, \alpha_4$. The resulting experimental coefficients are given in Table IV. Moreover, a $\chi^2$ analysis of the data was performed using the program CHIPLO.[16] This program compares the experimental angular distribution $W_E(\theta_i)$, with the theoretical angular distribution function $W_T(\theta_i)$, corresponding to a given spin hypothesis; the free parameters are the mixing ratios $\delta$ and the standard deviation $\sigma$ of the $m$ distribution, which is assumed to be Gaussian; $\sigma$ is varied between optional limits and $\arctan\delta$ between $\pm\pi/2$. The program finds the minimum of

$$\chi^2 = \frac{1}{N-R} \sum_i \frac{[W_E(\theta)_i - A_0(\delta) W_T(\theta_i)]^2}{\Delta^2_E(\theta_i)}, \qquad (2)$$

where $N$ is the number of angles and $R$ that of free parameters. $\Delta_E(\theta_i)$ is the experimental standard deviation of $W(\theta)$, and $A_0(\delta)$ is given by

$$A_0(\delta) = \frac{\sum_i W_E(\theta_i)}{\sum_i W_T(\theta_i)}. \qquad (3)$$

The spin hypothesis is rejected if the minimum $\chi^2$ lies above the 0.1%-confidence level of a $\chi^2$ distribution with $(N-R)$ degrees of freedom. In Fig. 2 some plots of the $\chi^2$ curves and of the $\chi^2 = \text{const}$ curves in the $\delta$-$\sigma$ plane are shown; the regions within the latter curves contain all points $(\sigma, \delta)$ which are consistent with the given spin hypothesis. (Dots denote the points where the 68%-confidence level is reached.) The correlation between $\delta$ and $\sigma$ often does not result in the usual elliptic but in a more "banana-like" shape of these $\chi^2$ valleys. In such cases a determination of $\delta$ is not possible without additional information about $\sigma$, i.e., about the alignment. Figure 3 shows a singles spectrum of the $^{81}\mathrm{Br}(\alpha, 2n)^{83}\mathrm{Rb}$ reaction taken at 125°.

## III. DISCUSSION OF THE $^{83}$Rb LEVEL SCHEME

The decay scheme of $^{83}$Rb constructed from $\gamma$-$\gamma$ coincidences, $\gamma$-excitation functions, and $\gamma$-angular distributions is shown in Fig. 4. Only levels and spin parity assignments which need further remarks are discussed

*The ground state and the 5.2 keV level.* Spin and parity of the ground state are $\frac{5}{2}^-$.[1,17] The existence of the 5.2 keV level[2,18] could be confirmed analyzing the decay of the 737.1 keV level.

*The 42.3 keV level.* No $\gamma$ decay of this $\frac{9}{2}^+$ isomeric state [$T_{1/2} \approx 7.8$ ms (Ref. 14)] established by Broda *et al.*[1] could be found.

*The 99.3 keV level.* We keep the $(\frac{3}{2}, \frac{1}{2})^-$ assignment of Ref. 14, although we prefer the latter, as Broda *et al.*[1] do also.

*The 389.2 keV level.* Our excitation function data are in agreement with the $I^\pi = \frac{3}{2}^-$ assignment of Broda *et al.*[1]

*The 423.5 keV level.* The $\frac{5}{2}^+$ assignment for this level is also taken from Broda *et al.*[1]

*The 564.7 keV level.* We can establish this level only from energy sum relations. Broda *et al.*[1] assigned $I^\pi = (\frac{3}{2}, \frac{5}{2})^-$. We make no assignments.

*The 737.1 keV level.* We could not find the 637.8 keV transition to the 99.3 keV level which is in the level scheme of Broda *et al.*[1] Its intensity could be estimated to be smaller than 0.1% of the 737.1 keV line. Their $(\frac{3}{2}^-, \frac{5}{2}^-)$ assignment is based on this line and in contradiction to our $\frac{7}{2}$ assignment which is based on our data of the remaining two lines. The parity is discussed with the next level.

*The 1103.0 keV level.* The 1098.4 keV line leading from this level to the $\frac{3}{2}^-$, 5.2 keV level reported by Broda *et al.*[1] could not be found in the spectrum coincident with the 999.2 keV line. Our data of the 1103.0 and the 365.7 keV line favor a $\frac{9}{2}$ assignment in contradiction to the $(\frac{3}{2}^-, \frac{5}{2}^-)$ assignment of Broda *et al.*[1] We propose negative parity for this level and for the 737.1 keV level as they only decay to negative parity states. Moreover, the observed branchings and the analogy to the $^{81}$Rb negative parity band[11] are arguments in favor of our spin and parity assignments.

*The 794.2 keV level.* This was not reported before (which suggests a high-spin state). In coincidence with the 182.0 keV line there are two cascades: 312.0–999.2–1103.0 keV and 1620.2–

TABLE III. List of gamma-gamma coincidences for the $^{81}Br(\alpha, 2n)^{83}Rb$ reaction. The intensities of the gamma transitions in the coincident spectra are given in parentheses. They were not corrected for the effect of the threshold in the constant fraction time pickoff system and for the efficiency of the gating detector. The intensity of the 100.5 keV line in the spectrum coincident with the 182.0 keV line is normalized to 100.

| Gate (keV) | Coincident gamma transitions (keV) |
|---|---|
| 94 | 290(9) |
| 101 | 182(45) 246(9) 286(9) 359(11) 362(11) 366(4) 405(7) [a] 543(4) 560(18) 737(4) 996(10) 1017(9) 1103(25) 1211(19) 1276(3) |
| 124 | 823(8) |
| 177 | 182(4) |
| 182 | 101(100) 104(12) 177(–) 208(9) 246(6) 312(43) 340(–) 362(67) 405(17) [a] 543(13) 560(–) [b] 601(10) 660(5) 737(12) 752(26) 996(22) 999(14) 1017(13) 1103(38) 1211(10) 1620(33) |
| 208 | 182(4) 1169(–) |
| 258 [b] | 101(–) 124(10) 276(8) [c] 286(4) 312(3) 405(4) |
| 286 | 101(12) 258(5) 312(4) |
| 290 [b] | 94(12) 276(5) [c] |
| 292 | 763(7) |
| 312 | 177(3) 182(28) 258(4) [b] 286(5) 348(3) 359(7) 362(10) 366(5) 999(18) 1103(12) |
| 340 | 182(4) 996(6) 1036(6) |
| 348 | 312(2) |
| 359 | 101(11) 312(5) |
| 362 | 101(15) 182(35) 312(7) 405(9) 601(6) 653(7) 752(–) 1149(9) |
| 366 | 101(4) 182(4) 312(4) 651(2) 732(2) 737(6) 999(5) 1211(–) |
| 381 [b] | 381(3) |
| 405 [b] | 101(3) 124(2) 182(8) 258(2) 312(–) 362(9) 743(7) [a] |
| 418 | 381(2) |
| 549 | 996(31) |
| 560 [b] | 101(16) 182(5) 276(5) [c] |
| 601 | 101(1) 182(3) 258(1) 362(4) |
| 653 | 362(5) 752(4) 1149(8) |
| 660 | 182(3) 732(2) |
| 732 | 101(1) 182(1) 560(1) 832(2) 1017(4) |
| 737 | 101(2) 124(2) 366(–) 560(2) 823(4) 1017(14) |
| 752 | 182(6) 362(3) 597(1) 630(1) 653(–) 970(13) 987(3) 1096(54) 1149(13) 1525(14) 1620(11) |
| 763 | 292(2) |
| 823 | 124(3) |
| 867 | 752(4) 970(4) 1096(4) |
| 906 | 996(3) |
| 970 | 752(12) 867(3) 1096(12) |
| 987 | 752(3) |
| 996 | 101(4) 182(4) 208(2) 340(–) 362(3) 549(15) 906(4) 1036(15) 1169(7) 1272(–) 1276(–) |
| 999 | 182(3) 312(5) 362(2) 366(2) 1103(10) |
| 1017 | 101(4) 124(3) 182(2) 348(–) 560(3) 660(2) 732(5) 737(10) 823(3) |
| 1036 | 340(–) 996(12) |
| 1055 | |
| 1096 | 752(32) 970(9) |
| 1103 | 101(6) 182(5) 312(3) 999(9) 1211(5) |
| 1149 | 362(4) 653(5) 752(13) |
| 1169 | 208(2) 996(6) |
| 1211 | 101(4) 182(1) 1103(–) |
| 1272 | 996(3) |
| 1276 | 101(2) 182(–) 996(–) |
| 1525 | 752(4) |
| 1544 | |
| 1620 | 182(3) 362(–) 752(4) |
| 1739 | |

[a] $^{207}Bi$. [b] Doublet. [c] $^{81}Br$.

751.9 keV. The difference of the energy sums suggests that the strong 751.9 keV line is placed on the $\frac{9}{2}^+$ state at 42.3 keV. This and the observed excitation function and angular distribution data lead to a $\frac{13}{2}^+$ assignment for the 794.2 keV level.

*The 805.0 keV level.* Our data are in agreement with the $\frac{7}{2}^+$ assignment of Broda *et al.*[1]

*The 1037.9 keV level.* This is populated by a strong 995.6 keV line. The two cascades coincident with the 100.5 keV line give the same arguments for the positioning of this line on the $\frac{9}{2}^+$ state at 42.3 keV as discussed for the 751.9 keV line. The intensity of the 995.6 keV line and the angular distribution and excitation function data suggest an $\frac{11}{2}$ assignment. This is in agreement with the missing of a decay to the $\frac{5}{2}^+$ state at 423.5 keV. Its intensity could be estimated to be smaller than 1.8% of the 995.6 keV line. We assume positive parity for this level because of the analogy to $^{81}$Rb (Ref. 11) and as no decay to negative parity states could be observed.

*The 1587.1 keV level.* The $(\frac{9}{2}, \frac{13}{2})$ assignment is based on the angular distribution data of the 549.0 keV transition. The excitation function favors $I = \frac{9}{2}$.

*The 1753.9 keV level.* $I = \frac{11}{2}$ is proposed from the excitation function of the 1016.8 and 651.1 keV transitions and from the abscence of transitions to other low-spin states, especially to the $\frac{5}{2}^-$ ground state. The branching ratios of the transitions to the $\frac{7}{2}^-$ and $\frac{9}{2}^-$ states and the fact that no transitions to positive parity states exist indicate negative parity.

*The 1890.2 keV level.* $I^\pi = \frac{17}{2}^+$ is proposed on the basis of the strong 1096.0–751.9 keV cascade, the angular distribution of the 1096.0 keV transition, and the excitation function of this line. This is also supported by the analogy to $^{81}$Rb (Ref. 11).

*The 1943.4 keV level.* The results of the angular distribution and excitation function of the 1149.2 keV transition and the observed branching ratios to the $\frac{13}{2}^+$ and $\frac{11}{2}^+$ give a $\frac{15}{2}^+$ assignment for this level.

*The 2074.0 keV level.* This is established by the 995.6–1036.1 keV coincidence. The angular distribution and excitation function data of the 1036.1 keV transition suggest a $(\frac{13}{2})$ spin for this level, which agrees with the fact that it is fed from a level at 2414.4 keV, which most likely has $I^\pi = (\frac{15}{2}^-)$ as will be shown later on.

*The 2102.2 keV level.* The excitation function of the 999.2 keV transition suggests an $(\frac{11}{2}, \frac{13}{2})$ spin. The $\frac{11}{2}$ assignment can be ruled out using the argument that if the 2102.2 keV level were a $\frac{11}{2}^-$ state, one would see a decay to the $\frac{7}{2}^-$ level at 737.1 keV, which has not been observed. Moreover, the branching to the $\frac{11}{2}^-$ state is weak. Therefore, we make a $\frac{13}{2}^-$ assignment.

*The 2206.6 keV level.* The spins $\frac{9}{2}$, $\frac{11}{2}$, and $\frac{13}{2}$ are possible from the angular distribution of the 1168.7 keV line. $(\frac{13}{2}, \frac{11}{2})$ seem to be more likely if we consider the excitation function and the feeding from the $(\frac{15}{2}^-)$ level at 2414.4 keV mentioned above.

*The 2314.1 keV level.* Spins $\frac{5}{2}$, $\frac{9}{2}$, and $\frac{13}{2}$ are possible from the angular distribution of the 1211.1 keV line. They are restricted to $\frac{9}{2}$, $\frac{13}{2}$ by its excitation function and by the observed transitions to the $\frac{11}{2}$ levels. A $\frac{9}{2}$ state which decays to an $\frac{11}{2}^-$ and $\frac{9}{2}^-$ levels should also decay to a $\frac{7}{2}^-$ level which is even lower in energy. Such a transition to the $\frac{7}{2}^-$ level at 737.1 keV was not observed, which rules out spin $\frac{9}{2}$. Hence, we propose a $(\frac{13}{2}^-)$ assignment for the 2314.0 keV level. The parity should be negative as a consequence of the branching ratio of the 1211.1 and 1275.9 keV transitions.

*The 2414.4 keV level.* This is depopulated by four $\gamma$ rays, the angular distributions and excitation functions of which suggest a $(\frac{15}{2})$ assignment for this level. Additionally, we can again argue that a tentative $\frac{11}{2}$ state which decays to the $\frac{13}{2}^-$ and $\frac{11}{2}^-$ states of one band should also decay to the low-lying $\frac{9}{2}^-$ (1103.0 keV) member of the same band. This was not observed. Since the 2414.4 keV level predominantly decays to negative parity states, we suggest negative parity. Moreover, a $(\frac{15}{2}^+)$ state should decay to the $\frac{11}{2}^+$ at 1034.9 keV. We could not find such a transition. Its relative intensity could be estimated to be smaller than 0.9% of the intensity of the 1620.2 keV transition to the $\frac{13}{2}^+$ state at 794.2 keV.

*The 2576.8 keV level.* From our excitation function and angular distribution measurements no spin and parity assignment can be made. The reasons why we can, however, assume a $(\frac{15}{2})$ spin for this level will be described in the discussion of the 2700.3 keV state.

*The 2700.3 keV level.* This is depopulated by two gamma rays, the angular distributions of which both have $\Delta I = \pm 1$ character. From the excitation function of the 285.9 keV transition spin $(\frac{17}{2})$ seems to be possible. This is supported by the fact that we observe no decay to other states with lower spins, but a feeding through a $\Delta I = \pm 1$ transition of 258.1 keV from a level of 2958.0 keV, which we assume to have $I = (\frac{19}{2})$. The $\Delta I = \pm 1$ transition to the 2576.9 keV state is the reason for assigning $(\frac{15}{2})$ to it.

## IV. DISCUSSION

The level scheme of $^{83}$Rb can be divided into three bands (Fig. 5).

TABLE IV. Energies, relative intensities, and angular distribution coefficients of gamma rays observed in the $^{80}$Se($^{6}$Li, 3$n$)$^{83}$Rb reaction at $E_{^{6}\mathrm{Li}} = 25$ MeV.

| $E_\gamma$ (keV) | $I_\gamma^{\mathrm{rel}}$ | $A_2/A_0$ | $A_4/A_0$ | $I_i \rightarrow I_f$ |
|---|---|---|---|---|
| 94.1 | 1.97 ± 0.14 | | | |
| 100.5 | 10.36 ± 0.27 | −0.235 ± 0.012 | −0.013 ± 0.016 | $(\frac{15}{2}) \rightarrow (\frac{13}{2})$ |
| 123.5 [a] | 10.41 ± 0.43 | −0.224 ± 0.011 | −0.007 ± 0.016 | $(\frac{17}{2}) \rightarrow (\frac{15}{2})$ |
| 176.7 | 0.66 ± 0.06 | | | |
| 182.0 | 18.61 ± 0.46 | −0.289 ± 0.008 | −0.005 ± 0.011 | $(\frac{17}{2}) \rightarrow (\frac{15}{2})$ |
| 207.7 | 1.99 ± 0.08 | | | |
| 258.1 [a] | 3.81 ± 0.12 | −0.347 ± 0.021 | −0.016 ± 0.028 | $(\frac{19}{2}) \rightarrow (\frac{17}{2})$ |
| 285.9 | 2.82 ± 0.12 | −0.274 ± 0.014 | 0.023 ± 0.017 | $(\frac{17}{2}) \rightarrow (\frac{15}{2})$ |
| 289.8 [a] | 4.87 ± 0.15 | | | |
| 291.5 [a] | 0.77 ± 0.07 | | | |
| 312.0 | 6.39 ± 0.19 | −0.341 ± 0.030 | 0.038 ± 0.043 | $(\frac{15}{2}) \rightarrow \frac{13}{2}$ |
| 340.3 | 1.21 ± 0.10 | | | |
| 348.3 | 1.43 ± 0.15 | | | |
| 358.7 | 3.43 ± 0.14 | −0.314 ± 0.047 | 0.003 ± 0.058 | $(\frac{13}{2}, \frac{17}{2}) \rightarrow (\frac{15}{2})$ |
| 362.2 | 10.89 ± 0.33 | −0.398 ± 0.015 | 0.014 ± 0.022 | $(\frac{19}{2}) \rightarrow (\frac{17}{2})$ |
| 365.7 [a] | 2.53 ± 1.18 | | | |
| 381.3 [a] | | | | |
| 389.2 [a] | 5.10 ± 0.18 | | | |
| 404.9 | 4.50 ± 0.19 | −0.574 ± 0.037 | 0.061 ± 0.052 | $(\frac{21}{2}) \rightarrow (\frac{19}{2})$ |
| 418.1 | 1.67 ± 0.18 | | | |
| 549.0 | 3.94 ± 0.32 | −0.630 ± 0.049 | 0.093 ± 0.069 | $(\frac{9}{2}, \frac{13}{2}) \rightarrow \frac{11}{2}$ |
| 559.5 [a] | | | | |
| 564.7 | 0.24 ± 0.22 | | | |
| 601.1 | | | | |
| 651.1 | 3.16 ± 0.18 | | | |
| 653.3 | 5.97 ± 0.26 | | | |
| 660.2 [a] | 3.33 ± 0.17 | | | |
| 731.9 | 5.63 ± 0.24 | 0.315 ± 0.019 | −0.065 ± 0.024 | $\frac{7}{2} \rightarrow \frac{3}{2}$ |
| 737.1 | 16.15 ± 0.53 | 0.450 ± 0.007 | 0.081 ± 0.008 | $\frac{7}{2} \rightarrow \frac{5}{2}$ |
| 751.9 | 100.0(p.def.) | 0.299 ± 0.010 | −0.069 ± 0.014 | $\frac{13}{2} \rightarrow \frac{9}{2}$ |
| 762.8 | 2.85 ± 0.28 | | | |
| 822.6 [a] | 5.29 ± 0.84 | | | |
| 867.3 | 3.12 ± 0.34 | | | |
| 905.5 | 3.71 ± 0.28 | | | |
| 970.2 | 16.34 ± 0.63 | 0.333 ± 0.012 | −0.092 ± 0.014 | $(\frac{21}{2}) \rightarrow \frac{17}{2}$ |
| 986.6 | 2.58 ± 0.20 | | | |
| 995.6 | 16.97 ± 0.93 | −0.755 ± 0.016 | 0.110 ± 0.023 | $\frac{11}{2} \rightarrow \frac{9}{2}$ |
| 999.2 | 13.65 ± 1.60 | | | |
| 1016.8 | 14.45 ± 0.51 | 0.256 ± 0.019 | 0.003 ± 0.024 | $\frac{11}{2} \rightarrow \frac{7}{2}$ |

TABLE IV. *(Continued).*

| $E_\gamma$ (keV) | $I_\gamma^{rel}$ | $A_2/A_0$ | $A_4/A_0$ | $I_i \rightarrow I_f$ |
|---|---|---|---|---|
| 1036.1 | 2.49 ± 0.17 | −0.744 ± 0.097 | 0.210 ± 0.139 | $(\frac{13}{2}) \rightarrow \frac{11}{2}$ |
| 1054.5 | 4.55 ± 0.21 | | | |
| 1096.0 | 46.01 ± 1.60 | 0.331 ± 0.012 | −0.040 ± 0.015 | $\frac{17}{2} \rightarrow \frac{13}{2}$ |
| 1103.0 | 26.37 ± 1.89 | 0.319 ± 0.021 | −0.077 ± 0.029 | $\frac{9}{2} \rightarrow \frac{5}{2}$ |
| 1149.2 | 11.22 ± 0.44 | −0.903 ± 0.014 | 0.157 ± 0.021 | $\frac{15}{2} \rightarrow \frac{13}{2}$ |
| 1168.7 | 3.03 ± 0.23 | −0.419 ± 0.055 | −0.068 ± 0.076 | $(\frac{13}{2}, \frac{11}{2}) \rightarrow \frac{11}{2}$ |
| 1211.1 | 5.75 ± 0.26 | 0.320 ± 0.032 | −0.107 ± 0.040 | $(\frac{13}{2}) \rightarrow \frac{9}{2}$ |
| 1272.1 | 2.22 ± 0.17 | | | |
| 1275.9 | 1.59 ± 0.16 | | | |
| 1524.5 | 4.60 ± 0.24 | | | |
| 1544.8 | 5.00 ± 0.32 | | | |
| 1620.2 | 5.03 ± 0.28 | | | |
| 1738.5 | 3.11 ± 0.35 | | | |

[a] The values of the line were obtained from the analysis of the $^{81}$Br$(\alpha, 2n)^{83}$Rb reaction data.

### A. The positive parity states

The positive parity state Fig. 5(a) result from an excited particle in the $1g_{9/2}$ shell coupled to the core. They show simple decoupling features, i.e., the lowest positive parity state has spin $I^\pi = \frac{9}{2}^+$ which corresponds to the spin of the spherical single-particle state $1g_{9/2}$. The decoupled band $I = j, j+2, j+4, \ldots$ is built on the lowest positive parity state and the energy differences of these states are almost equal to those of the ground state band in the adjacent even mass nucleus $^{82}$Kr. The occurrence of decoupled bands in deformed nuclei is due to the Coriolis interaction and can be understood in the framework of the model of Stephens.[8]

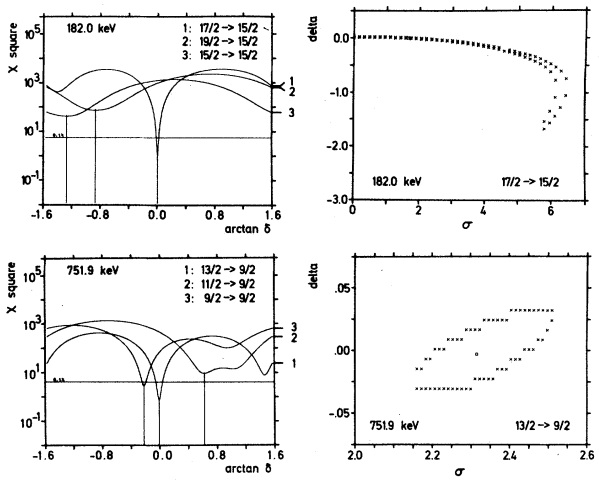


FIG. 2. Chi-square analysis of some of the angular distribution data from the reaction $^{80}$Se$(^6$Li$, 3n)^{83}$Rb (see text).

#### *1. Symmetric rotor calculations*

We used the program ODDROT, which is a revised version[19] of the ABPF program of Hird and Huang.[20] ODDROT solves the Schrödinger equation of the quasiparticle coupled to an axially symmetric rotor, which diagonalizes step by step the Hamiltonian

$$H = H_{\text{spherical}} + V_{\text{deformed}} + V_{\text{pairing}} + H_{\text{rotor}} . \quad (4)$$

The parameters of the spherical potential (Woods-Saxon) were chosen so as to reproduce the single-particle spectrum calculated by Reehal and Sorenson[21] for $\beta = 0$. The deformation parameters $\beta_2$ and $\beta_4$ of the Nilsson operator $V_{\text{deformed}}$ are free. In our calculations we took $\beta_4 = 0$ and adjusted $\beta_2$ to the $B(E2; 2_1^+ \rightarrow 0^+_{\text{g.s.}})$ value of the neighboring even-even nucleus. The pairing term is treated by the BCS procedure without blocking and $\Delta$ is calculated from the odd-even mass difference. The Fermi energy $\lambda_F$ is a free parameter. The so-called recoil term, which is important at weak deformations, was calculated in accordance with Ref. 22. Since the nuclei in this region are

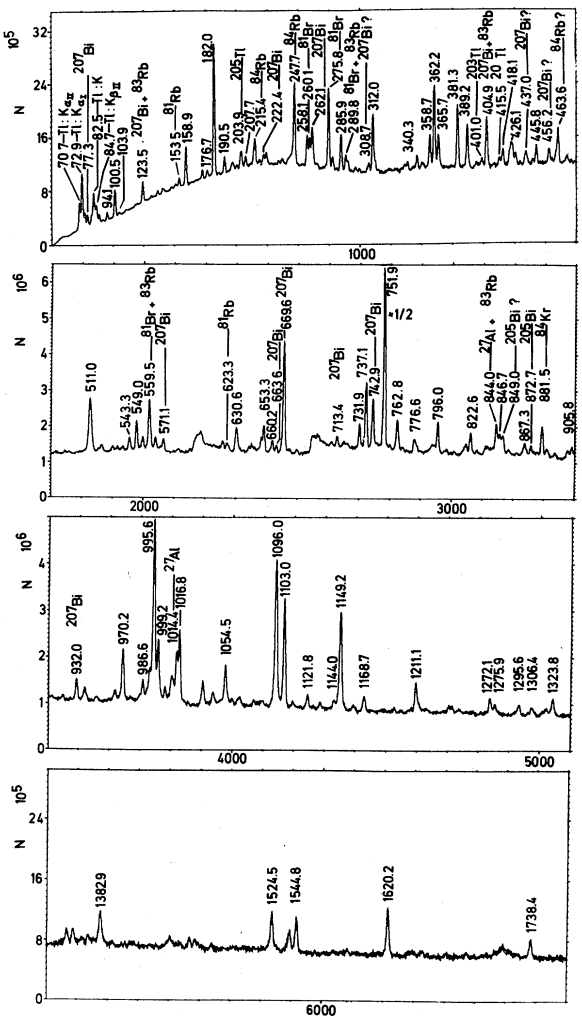

FIG. 3. Singles spectrum of the reaction $^{81}$Br$(\alpha, 2n)^{83}$Rb taken at 125°. $N(10^6)$ is the number of counts per channel multiplicated with the channel number.

rather soft, two parametrizations of the moment of inertia can be introduced into $H_{\text{rotor}}$, viz., either the usual expansion into powers of $I(I+1)$ or the variable moment of inertia (VMI) approximation.[23]

For the calculation of the positive parity states we used the first parametrization of the moment of inertia in $H_{\text{rotor}}$. The two expansion coefficients were fitted to the experimental spectrum. With the VMI approximation we were not able to reproduce the experimental fact that the $\frac{5}{2}^+$ state lies above the $\frac{9}{2}^+$. This probably happens because in minimizing the rotational energy only the diagonal element of the strong Coriolis energy is taken into account. The Coriolis operator was attenuated by the factor $\eta = 0.9$.

In Fig. 6 the result of our calculations is compared with the experimental data. The corresponding wave functions confirm the decoupled character of the positive parity band. Table V shows, that the Nilsson states with small values of $K = \Omega$ are dominating the wave functions of the favored states, and Table VI shows that these states are almost pure $1g_{9/2}$ states. On the other hand, the fit is rather bad for the nonyrast levels. The small energy differences between favored and unfavored states, as well as the presence of additional low-lying positive parity states with spins ($\frac{9}{2}$, $\frac{11}{2}$, and $\frac{13}{2}$), cannot be reproduced by the symmetric rotor calculations. This indicates that an additional degree of freedom such as static or dynamic triaxial deformation is needed in $^{83}$Rb. This is also supported by the experimental features of the even-even $^{82}$Kr core, where low-lying second $2^+$ and $3^+$ states could be observed[12,14] and the $E_{4^+_1}/E_{2^+_1}$ ratio is intermediate between the harmonic vibrator and the triaxial rotor limit.

### 2. *Asymmetric rotor calculations*

These were carried out for the positive parity states with the model ARO II of Toki and Faessler.[25] This model couples an odd particle occupying two different $j$ shells to a $\gamma$-deformed soft core. The VMI parameters are fixed by the experimental spectrum of the core. The remaining free parameters of this model are EDIF, $\Delta$, $\beta$, $\gamma$, and $\lambda_F$. EDIF is the energy difference of the spherical states $g_{9/2} - d_{5/2}$ which is taken from the Nilsson scheme. The energy gap $\Delta$ is calculated from the odd-even mass difference. The $\beta$ deformation is extracted from the $B(E2, 2^+ \to 0^+)$ value and the $\gamma$ deformation—according to the Davydow model—from the $E_{2^+_1}/E_{2^+_2}$ energy ratio of the even $^{82}$Kr core. The Fermi energy $\lambda_F$ is estimated from the Nilsson scheme.

Figure 7 shows the result of our calculation. The good agreement confirms the great importance of the additional $\gamma$ degree of freedom for the positive parity states of $^{83}$Rb. Similar conclusions were drawn by Toki and Faessler[26] from their calculations of the $^{81}$Rb positive parity states. For this nucleus, the RAC picture is also supported by the measured ratios $R_1 = B(E2, \frac{13}{2} \to \frac{9}{2})/B(E2, 2 \to 0)_{\text{core}} = 1.43 \pm 0.02$ and $R_2 = B(E2, \frac{17}{2} \to \frac{13}{2})/B(E2, \frac{13}{2} \to \frac{9}{2}) = 1.47 \pm 0.29$, for which the Coriolis coupling model gives $R_1 = 1.5$ and $R_2 = 1.23$, respectively, when $\gamma = 25°$.[27] In $^{83}$Rb lifetimes have not yet been measured.

### B. The negative parity states

For the negative parity states Fig. 5(b) the situation is more complicated because they are

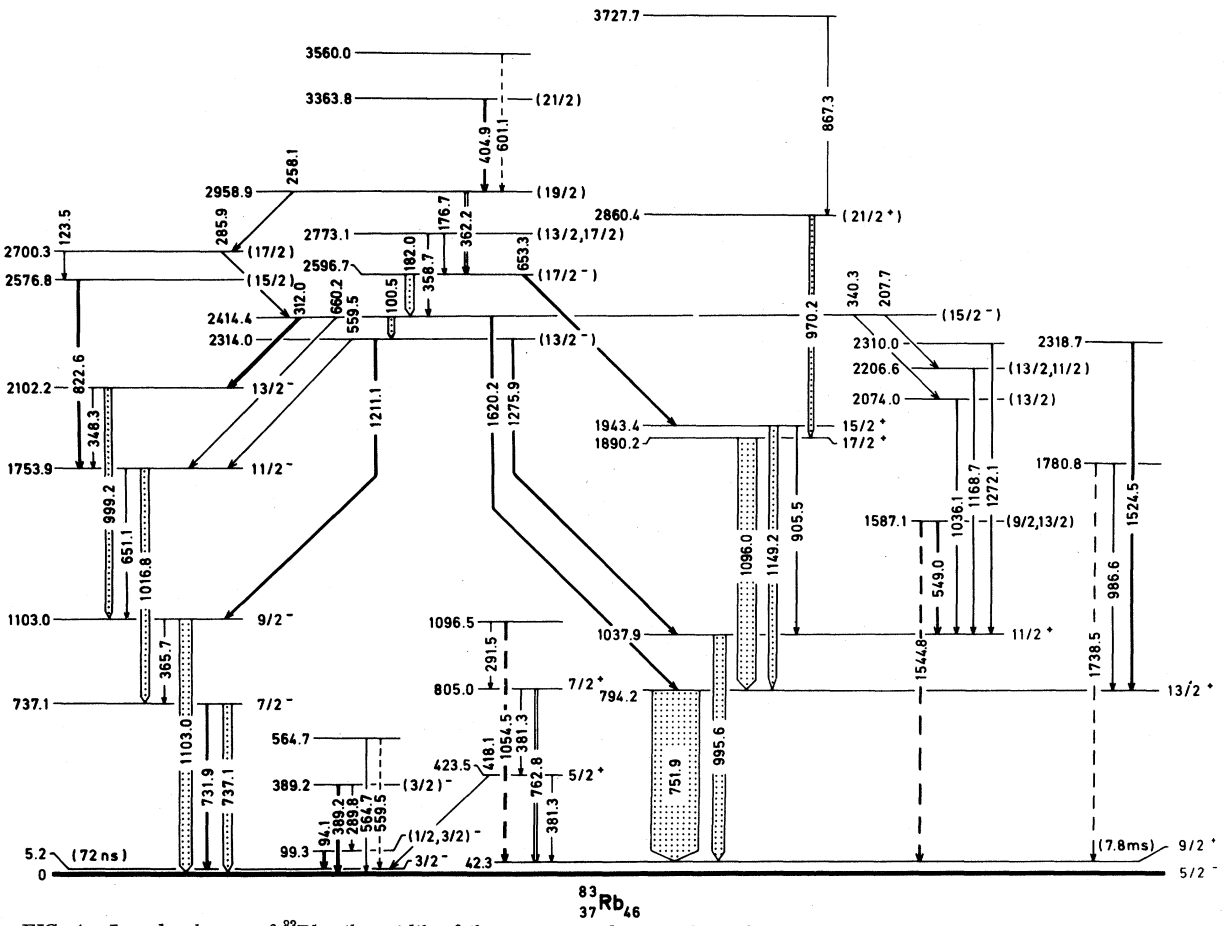


FIG. 4. Level scheme of $^{83}$Rb; the width of the arrows indicates the relative intensities of the lines. Hatched lines indicate transitions which were not confirmed by coincidences.

constructed on the basis of the $2p_{3/2}$, $1f_{5/2}$, and $2p_{1/2}$ shell model states which are strongly mixed in the deformed potential. Nevertheless, they show the same close analogy to the corresponding negative parity bands in $^{77}$Br (Ref. 9) and $^{81}$Rb (Ref. 11) as was observed for the positive parity states.

### *1. Symmetric rotor calculations*

The symmetric rotor plus quasiparticle Hamiltonian (4) was diagonalized for the negative parity states of $^{83}$Rb to obtain a closer insight into their nature. We used the program ODDROT mentioned above with essentially the same choice of parameters as for the calculation of the positive parity states, but with the difference that the moment of inertia was now parametrized according to the VMI approximation.[23] Hence, the model is called SRVMI in the following. One difficulty should be mentioned: In $^{83}$Rb the $\frac{5}{2}^-$ state is lowered below the $\frac{3}{2}^-$ state which is the ground state in $^{81}$Rb. Scholz and Malik[7] explained it as being due to the blocking effect. In our interpretation it is a Coriolis effect due to a strong admixture of the $\frac{1}{2}^-$ [310] orbital. We can obtain this strong Coriolis mixing in our calculations by increasing slightly the stiffness parameter $C$ over the value which optimizes the fit of the high-spin levels. In order to compensate the negative effects, an additional inertial parameter $\theta_{ok}$ for the $\frac{5}{2}^-$ [303] orbital has to be incorporated into the calculations.

The resulting amplitudes of the main components in the wave functions for each spin are listed in Table VII; the corresponding energies are compared with the experimental data in Fig. 8. The most interesting features are as follows: The dominant components of the wave functions are given by the Nilsson orbitals with $K=\frac{1}{2}$, $\frac{3}{2}$, and $\frac{5}{2}$. The weights of the components do not stay constant along the band but display regular oscillations. This is caused by the admixture of the $\frac{1}{2}^-$ [310] orbital. A similar situation was found in

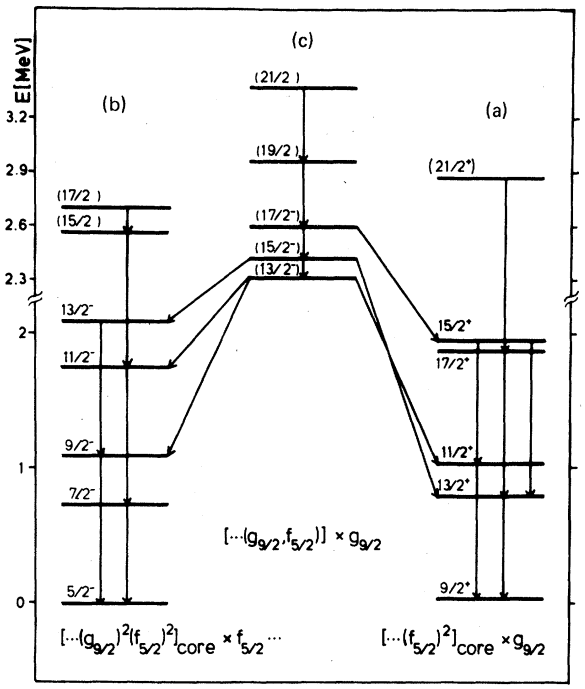


FIG. 5. Structure of the $^{83}$Rb level scheme.

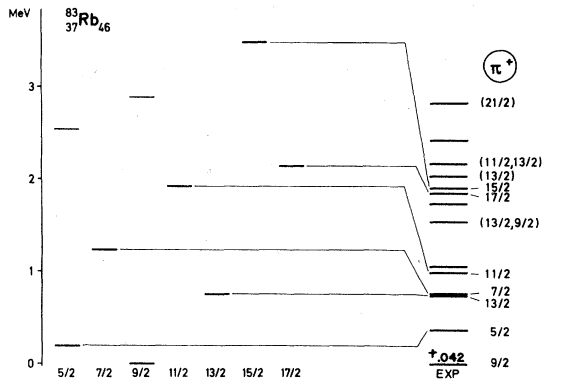


FIG. 6. Symmetric rotor calculations for $^{83}$Rb positive parity states compared with the experimental data. $\lambda_F = -10.8$ MeV, $\Delta = 1.86$ MeV, $A = 0.15$ MeV, $B = -0.00025$ MeV, $\beta = 0.21$, $\eta = 0.9$.

our calculations for the $^{77}$Br and $^{81}$Rb negative parity states (see also Ref. 19), where the same kind of staggering is known from the experimental spectra.

The results of the $^{81}$Rb calculations are, however, in disagreement with those of the earlier published work of Friederichs *et al.*,[11] in which the phase of oscillation of the $\frac{1}{2}^-$ [310] component is shifted by $\hbar$ and where the $\frac{3}{2}^-$ [312] component is dominant in the wave function of the $\frac{3}{2}^-$ ground state. On the other hand, our results are supported by the measurement of magnetic moments, recently carried out by Ekström *et al.*[28] who suggested a $\frac{3}{2}^-$ [301] assignment for the $\frac{3}{2}^-$ ground state of $^{81}$Rb.

Owing to the low particle angular momentum $j$ and since we do not deal with a single $j$ shell, the Coriolis force in the negative parity band is not strong enough to decouple completely the motion of the odd particle from the core; that is, the situation comes nearer to the strong coupling limit than to the decoupled one in contrast to the positive parity band. This is the reason why in the calculations of the negative parity states the VMI approximation works much better than in those of the positive parity band; as we observe only the ground band for the negative parity levels, the effects of triaxiality are hardly noticeable, too. In this way, the symmetric rotor model with a variable moment of inertia provides a rather good description of the $^{83}$Rb negative parity ground band states.

### 2. *The negative parity levels at high energy*

The structure of the $^{83}$Rb negative parity states suddenly changes at about 2.3 MeV Fig. 5(c). A new band of relative strong $\Delta I = 1$, low energy transitions occurs, starting with $I^\pi = \frac{13}{2}^-$. A pos-

TABLE V. Level energies and coefficients of the dominant components in the wave functions of the $^{83}$Rb positive parity states, calculated from the symmetric rotor model. $\lambda_F = -10.8$ MeV, $\Delta = 1.86$ MeV, $\beta = 0.21$, $A = 0.15$ MeV, $B = 0.25 \times 10^{-3}$ MeV, $\eta = 0.9$.

| | | | $K_\nu[N, n_z, \Lambda]$ | | | | |
|---|---|---|---|---|---|---|---|
| $I^\pi$ | $E_{exp.}$ | $E_{calc.}$ | $\frac{1}{2}_5$ [440] | $\frac{3}{2}_3$ [431] | $\frac{5}{2}_2$ [422] | $\frac{7}{2}_1$ [413] | $\frac{9}{2}_1$ [404] |
| $\frac{9}{2}^+$ | (0.042) | 0.0 | 0.713 | 0.580 | 0.355 | 0.143 | 0.029 |
| $\frac{13}{2}^+$ | 0.752 | 0.757 | 0.696 | 0.576 | 0.373 | 0.172 | 0.048 |
| $\frac{17}{2}^+$ | 1.848 | 2.142 | 0.690 | 0.574 | 0.378 | 0.183 | 0.055 |

TABLE VI. Contributions of the different $j$ shells to the five Nilsson states which give the dominant amplitudes in the wave function of the decoupled states (Table VII).

| $N$ | $l$ | $j$ | $\frac{1}{2}_5$ [440] | $\frac{3}{2}_3$ [431] | $\frac{5}{2}_2$ [422] | $\frac{7}{2}_1$ [413] | $\frac{9}{2}_1$ [404] |
|---|---|---|---|---|---|---|---|
| 0 | 0 | $\frac{1}{2}$ | 0.0022 | 0.0 | 0.0 | 0.0 | 0.0 |
| 2 | 0 | $\frac{1}{2}$ | 0.0167 | 0.0 | 0.0 | 0.0 | 0.0 |
| 4 | 0 | $\frac{1}{2}$ | 0.0495 | 0.0 | 0.0 | 0.0 | 0.0 |
| 2 | 2 | $\frac{3}{2}$ | 0.0015 | −0.0003 | 0.0 | 0.0 | 0.0 |
| 2 | 2 | $\frac{5}{2}$ | −0.1722 | −0.1448 | −0.0921 | 0.0 | 0.0 |
| 4 | 2 | $\frac{3}{2}$ | 0.0136 | 0.0149 | 0.0 | 0.0 | 0.0 |
| 4 | 2 | $\frac{5}{2}$ | −0.3089 | −0.2598 | −0.1712 | 0.0 | 0.0 |
| 4 | 4 | $\frac{9}{2}$ | 0.9338 | 0.9546 | 0.9809 | 1.0000 | 1.0000 |

sible interpretation of this band assumes a change of the intrinsic structure of the even-even core $^{82}$Kr. In this nucleus, above about 2.4 MeV, negative parity states with $I=(3^-)$, $4^-$, and $5^-$ exist.[29,30] Generally, negative parity states can be created from two quasiparticle states, where one quasiparticle occupies the unique parity high-spin orbit while the other moves in one of the low-spin orbits of opposite parity. In $^{82}$Kr these should be the $g_{9/2-}$ and the $p_{1/2-}$, $p_{3/2-}$, or $f_{5/2-}$ shells, respectively.[31] Possible configurations are $(p_{3/2})\otimes(g_{9/2})$ and $(f_{5/2})\otimes(g_{9/2})$. Thus, one can get negative parity states with spins $3^-\leq I^\pi\leq 6^-$ or $2^-\leq I^\pi\leq 7^-$. Bands based on a $3^-$ state have also been observed in the even-even Sr isotopes.[32] In $^{83}$Rb which has one more proton, an additional $g_{9/2-}$ quasiparticle has to be coupled to the 2qp

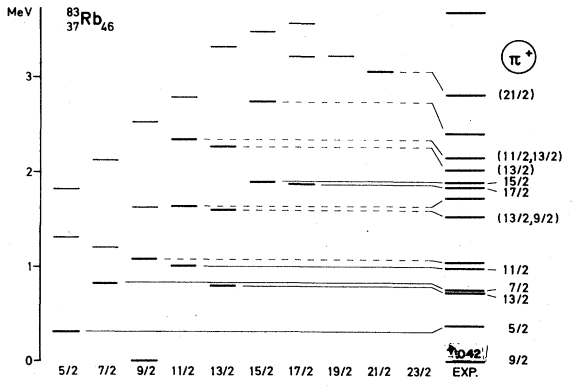


FIG. 7. Asymmetric rotor calculations for $^{83}$Rb positive parity states compared with the experimental data. $\lambda_F=-3.4$ MeV, $\Delta=1.87$ MeV, $\beta=0.25$, $\gamma=28°$, EDIF $=4.5$ MeV.

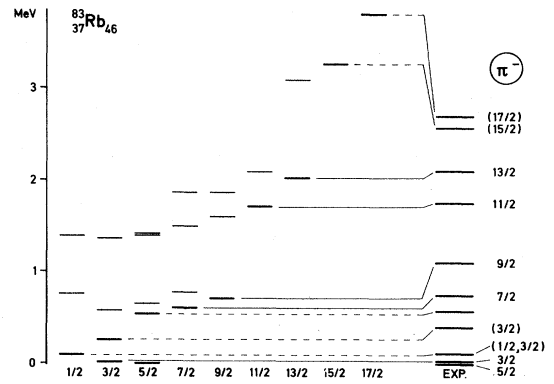


FIG. 8. Symmetric rotor calculations for $^{83}$Rb negative parity states. $\lambda_F=-10.8$ MeV, $\Delta=1.86$ MeV, $\beta=0.21$, $C=0.45$ MeV$^3$.

states of the core yielding configurations like $[\ldots(f_{5/2},g_{9/2})]_{\text{core}}\otimes g_{9/2}$; in this configuration, as an example, an $f_{5/2}$ pair of the core is broken and one particle is lifted up into the $g_{9/2}$ orbit. The broken pair and the additional $g_{9/2}$ proton then represent the 3qp configuration. A new band is built on this 3qp configuration which crosses the decoupled 1qp band of $^{83}$Rb at about 2.3 MeV (Fig. 9).

It should be pointed out that since the information about the anomalous negative parity states in $^{82}$Kr as well as in $^{83}$Rb is still very meager and since no three-quasiparticle-plus-rotor model exists, this attempt to describe these states is rather tentative. On the other hand, negative parity bands based on a $5^-$ state have been observed in Pd, Ba, Ce, and Er, as well as in the Pt-Hg region. These bands have been described in the framework of the rotor-plus-two-quasi-

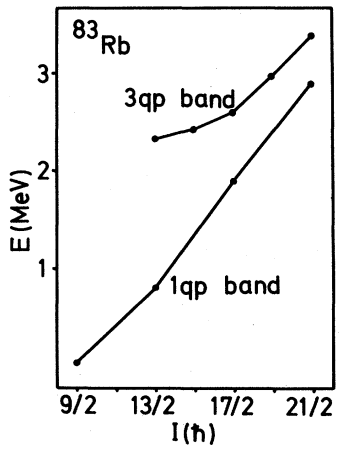


FIG. 9. The three-quasiparticle band and the one-quasiparticle band in $^{83}$Rb.

TABLE VII. Level energies and coefficients of the dominant components in the wave functions of the $^{83}$Rb negative parity states, calculated from the symmetric rotor model including VMI. $\lambda_F = -10.8$ MeV, $\Delta = 1.86$ MeV, $\beta = 0.21$, $C = 0.45$ MeV$^3$.

| | | | $K_\nu[N, n_z, \lambda]$ | | | | | |
|---|---|---|---|---|---|---|---|---|
| $I^\pi$ | $E_{calc.}$ | $E_{exp.}$ | $\frac{1}{2}_6$ [301] | $\frac{1}{2}_5$ [321] | $\frac{1}{2}_4$ [310] | $\frac{3}{2}_4$ [301] | $\frac{3}{2}_3$ [312] | $\frac{5}{2}_2$ [303] |
| $\frac{1}{2}^-$ | 0.085 | 0.099 | 0.137 | 0.978 | 0.159 | | | |
| $\frac{3}{2}^-$ | 0.005 | 0.005 | 0.101 | −0.613 | 0.167 | 0.752 | 0.145 | |
| $\frac{5}{2}^-$ | 0.0 | 0.0 | 0.215 | 0.610 | 0.299 | −0.405 | 0.482 | 0.309 |
| $\frac{7}{2}^-$ | 0.600 | 0.737 | −0.020 | 0.477 | −0.056 | −0.544 | 0.343 | 0.596 |
| $\frac{9}{2}^-$ | 0.706 | 1.103 | 0.224 | 0.538 | 0.339 | −0.346 | 0.500 | 0.419 |
| $\frac{11}{2}^-$ | 1.711 | 1.754 | 0.035 | 0.267 | 0.045 | −0.368 | 0.440 | 0.772 |
| $\frac{13}{2}^-$ | 2.024 | 2.102 | 0.213 | 0.483 | 0.339 | −0.319 | 0.493 | 0.511 |
| $\frac{15}{2}^-$ | 3.273 | 2.577 | 0.045 | 0.181 | 0.071 | −0.295 | 0.422 | 0.834 |

pariticle model by Flaum and Cline (axially symmetric rotor)[33,34] and by Toki and Faessler ($\gamma$-deformed rotor),[35] or in the semidecoupled approximation of Neergard, Vogel, and Radomski.[36] Three-quasiparticle states of the same nature have also been observed.[37] Since there is a strong similarity between the $1h_{11/2}$ and the $1g_{9/2}$ shells, it will be interesting to search for two- or three-quasiparticle states with negative parity in the Kr-Sr region.

## ACKNOWLEDGMENTS

We are indebted to Professor K. P. Lieb for various useful discussions and to A. Dewald, A. Geuer, D. Hippe, H. W. Peters, and H. W. Schuh for their collaboration during the experiments. This work was supported by the German Bundesministerium für Forschung und Technologie.

[1] R. Broda, A. Z. Hrynkiewicz, J. Styczen, and W. Walus, Nucl. Phys. A216, 493 (1973).
[2] R. C. Etherton, L. M. Beyer, W. H. Kelly, and D. J. Horen, Phys. Rev. 168, 1249 (1968).
[3] T. Paradellis and S. Hontzeas, Can. J. Phys. 49, 1750 (1971).
[4] K. Krishan, S. K. Basu, and S. Sen, Phys. Rev. C 13, 2055 (1976).
[5] F. Ackermann, J. Platz, and G. zu Pulitz, Z. Phys. 260, 87 (1973).
[6] A. Winnacker, Ph. D. dissertation, Heidelberg, 1970.
[7] W. Scholz and F. B. Malik, Phys. Rev. 176, 1355 (1968).
[8] F. S. Stephens, R. M. Diamond, and S. G. Nilsson, Phys. Lett. 44B, 429 (1973).
[9] M. A. Deleplanque, C. Gerschel, N. Perrin, B. Alder, and M. Ishihara, Phys. Lett. 35, L-237 (1974).
[10] B. Heits, H.-G. Friederichs, A. Rademacher, K. O. Zell, C. Protop, and P. von Brentano, Phys. Rev. C 15, 1742 (1977).
[11] H.-G. Friederichs, A. Gelberg, B. Heits, K. O. Zell, and P. von Brentano, Phys. Rev. C 13, 2247 (1976).
[12] J. Hadermann and A. C. Rester, Nucl. Phys. A231, 120 (1974).
[13] H. W. Schuh, Ph. D. dissertation, Köln, 1980.
[14] J. F. Lemming and D. C. Kocher, Nucl. Data Sheets 15, 150 (1975); 15, 188 (1975).
[15] H. W. Schuh, Ph. D. dissertation, Köln, 1980.
[16] F. Paar, Köln, 1979 (unpublished).
[17] J. P. Hobson, J. C. Hubbs, W. A. Nierenberg, H. B. Silsbee, and R. J. Sunderland, Phys. Rev. 104, 101 (1956).
[18] S. Morinobu and H. Ikegami, Nucl. Phys. A189, 170 (1972); S. Morinobu, I. Katayama, H. Adachi, M. Ishii, and H. Ikegami, in Proceedings of the International Conference on Nuclear Structure, Tokyo, Japan, Contributed Papers, published in J. Phys. Soc. Jpn. Suppl. 24, 169 (1967).
[19] U. Kaup, Köln, 1978 (unpublished).
[20] K. Hird and K. Huang, Comput. Phys. Commun. 9, 293 (1975).
[21] B. S. Reehal and R. A. Sorensen, Phys. Rev. C 2, 819 (1970).
[22] E. Osnes, J. Rekstad, and O. K. Gjøtterud, Nucl. Phys. A253, 45 (1975).
[23] G. Scharff-Goldhaber, C. B. Dover, and A. L. Goodman, Annu. Rev. Nucl. Sci. 26, 239 (1976).
[24] M. Sakai, At. Data Nucl. Data Tables 15, 513 (1975).
[25] H. Toki and A. Faessler, Nucl. Phys. A253, 231 (1975).
[26] H. Toki and A. Faessler, Phys. Lett. 63B, 121 (1976).
[27] J. Panqueva, H. P. Hellmeister, F. J. Bergmeister, and K. P. Lieb, *Structure of Medium-Heavy Nuclei, 1979,* Institute of Physics Conference Series No. 49, 235 (1980).
[28] C. Ekström, S. Ingelmann, and G. Wannberg (unpublished).

[29]D. G. McCauley and J. E. Draper, Phys. Rev. C 4, 475 (1971).
[30]S. Matsuki, N. Sakamoto, K. Ogino, Y. Kadota, Y. Saito, T. Tanabem, M. Yasue, and Y. Okuma, Phys. Lett. 72B, 319 (1978).
[31]G. R. Meredith and R. A. Meyer, Nucl. Phys. A142, 513 (1970).
[32]J. B. Ball and J. J. Pinajian, Phys. Rev. C 8, 1438 (1973).
[33]C. Flaum, D. Cline, A. W. Sunyar, O. C. Kistner, Y. K. Lee, and J. S. Kim, Nucl. Phys. A264, 291 (1976).
[34]C. Flaum and D. Cline, Phys. Rev. C 14, 1224 (1976).
[35]H. Toki, K. Neergard, P. Vogel, and A. Faessler, Nucl. Phys. A279, 1 (1977).
[36]K. Neergard, P. Vogel, and M. Radomski, Nucl. Phys. A238, 199 (1975).
[37]J. Gizon, A. Gizon, M. R. Maier, R. M. Diamond, and F. S. Stephens, Nucl. Phys. A222, 557 (1974).